

Multimeric structure of CIC-1 chloride channel revealed by mutations in dominant myotonia congenita (Thomsen)

Klaus Steinmeyer, Claudius Lorenz, Michael Pusch, Manuela C.Koch¹ and Thomas J.Jentsch²

Centre for Molecular Neurobiology (ZMNH), Hamburg University, Martinistrasse 52, D-20246 Hamburg, Germany and ¹Medical Centre for Human Genetics, Marburg University, Bahnhofstrasse 7a, D-35037 Marburg, Germany

²Corresponding author

Communicated by H.Betz

Voltage-gated CIC chloride channels play important roles in cell volume regulation, control of muscle excitability, and probably transepithelial transport. CIC channels can be functionally expressed without other subunits, but it is unknown whether they function as monomers. We now exploit the properties of human mutations in the muscle chloride channel, CIC-1, to explore its multimeric structure. This is based on analysis of the dominant negative effects of CIC-1 mutations causing myotonia congenita (MC, Thomsen's disease), including a newly identified mutation (P480L) in Thomsen's own family. In a co-expression assay, Thomsen's mutation dramatically inhibits normal CIC-1 function. A mutation found in Canadian MC families (G230E) has a less pronounced dominant negative effect, which can be explained by functional WT/G230E heterooligomeric channels with altered kinetics and selectivity. Analysis of both mutants shows independently that CIC-1 functions as a homooligomer with most likely four subunits.

Key words: anion channel/muscle/myotonia/human genetics/voltage-gated

Introduction

Chloride channels are expressed in the plasma membrane of virtually every animal cell and participate in various functions. Expression cloning of CIC-0, the voltage-gated chloride channel from *Torpedo* electric organ (Jentsch *et al.*, 1990), led to the molecular identification of several mammalian members of this gene family. CIC-1 is the major skeletal muscle chloride channel and ensures the electrical stability of the muscle (Steinmeyer *et al.*, 1991a,b). CIC-2 is ubiquitously expressed (Thiemann *et al.*, 1992) and participates in cell volume regulation (Gründer *et al.*, 1992). Finally, CIC-K1 is predominantly expressed in the kidney and may be involved in transepithelial transport (Uchida *et al.*, 1993).

CIC chloride channels are structurally unrelated to any other known class of ion channels. First insights into structure–function relationships are available for the activation of CIC-2 by increases in cell volume (Gründer *et al.*, 1992). While the single CIC-0 cDNA is sufficient for the expression of the fully functional double-barrelled

Torpedo channel (Bauer *et al.*, 1991), it is still unclear whether CIC channels function as monomers or homooligomers.

In principle, the multimeric structure of a channel protein can be investigated by electron microscopy of the purified protein (Unwin *et al.*, 1988) or by biochemical methods such as chemical crosslinking (Langosch *et al.*, 1988), but both approaches may be difficult. Functional co-expression of wild-type (WT) toxin-sensitive and mutant toxin-insensitive Shaker potassium channel subunits was used to deduce a tetrameric structure for that channel family (MacKinnon, 1991), and a similar analysis was used for an acetylcholine receptor (Cooper *et al.*, 1991). In this work, we use a novel approach by analysing in detail the functional effects of human CIC-1 mutations in dominant myotonia congenita (MC).

Dominant inheritance is easily explained with gain-of-function mutations. For instance, mutations in the sodium channel cause additional late sodium currents in dominant paramyotonia congenita or hyperkalemic periodic paralysis (Ptaček *et al.*, 1991; Rojas *et al.*, 1991; McClatchey *et al.*, 1992; Cannon and Strittmatter, 1993; Cummins *et al.*, 1993). This slightly depolarizes muscle membranes after action potentials, resulting in muscle hyperexcitability. Loss-of-function mutations can lead to a dominant phenotype by a gene dosage effect if 50% of the gene product (supplied by the normal allele) is not sufficient for normal function. Alternatively, dominant effects can be explained by a mechanism in which the mutant protein can bind to the protein and, by doing so, inactivates it (Müller-Hill *et al.*, 1968; Gisselmann *et al.*, 1989). The extent of inactivation will depend on the number of subunits in the oligomer: if a single subunit suffices to destroy the function of the complex, a higher stoichiometry of the multimer should lead to a more pronounced inhibition. Since both recessive and dominant forms of myotonia were linked to the CIC-1 chloride channel (Koch *et al.*, 1992), we expected that such a dominant negative effect is the basis for the pattern of inheritance observed with MC. Thus, analysis of MC mutations may clarify the multimeric structure of CIC channels.

Autosomal dominant MC was first described by Thomsen (1876). He himself suffered from the disease, which has come to bear his name (Thomsen's disease). In contrast, generalized myotonia (GM) is recessively inherited (Becker, 1977). Myotonia is due to an instability of the muscle membrane potential, resulting in repetitive electrical activity of muscle fibres after voluntary contraction (Rüdel and Lehmann-Horn, 1985).

Skeletal muscle has an unusually high chloride conductance which is essential for the repolarization after action potentials (Bretag, 1987; Rüdel and Lehmann-Horn, 1985). *In vitro* studies have revealed a decreased chloride conductance in myotonic muscles of humans (Lipicky *et al.*, 1971; Rüdel *et al.*, 1988; Franke *et al.*, 1991), goats (Bryant

and Morales-Aguilera, 1971) and mice (Mehrke *et al.*, 1988). Steinmeyer *et al.* (1991b) recently demonstrated that the CIC-1 chloride channel is inactivated by transposon insertion in a recessive myotonic mouse strain. Subsequently, genetic linkage of both forms of human myotonia to CIC-1 and to the nearby marker TCRB was demonstrated (Koch *et al.*, 1992). Linkage to TCRB has also been reported for Canadian MC families (Abdalla *et al.*, 1992), and mutations associated with GM (F413C) (Koch *et al.*, 1992) and MC (G230E) (George *et al.*, 1993) have been found.

We have now identified a missense mutation (P480L) in Thomsen's own family. Functional analysis in *Xenopus* oocytes of this and the G230E mutation shows that both destroy normal channel activity and exert dominant negative effects on wild-type (WT) channels. The extent of inhibition is less pronounced with G230E due to the formation of functional WT/mutant channels with altered properties. In addition to proving unambiguously the role of CIC-1 in dominant myotonia, this shows that CIC channels function as oligomers with more than two (and probably four) identical subunits.

Results

Identification of missense mutations in Thomsen's disease

The human CIC-1 coding sequence is interrupted by 22 introns (C.Lorenz, K.Steinmeyer and T.J.Jentsch, in preparation) with some correlation with putative transmembrane domains (Figure 1A). Intronic primers were used to sequence exons on genomic CIC-1 clones obtained from a member of Thomsen's own family. We identified two deviations from normal human CIC-1 (hCIC-1) sequence. A point mutation in exon 8 results in a replacement of an arginine by glutamine between putative transmembrane domains D5 and D6 (R300Q), and a mutation in exon 13 on the other allele causes a proline to leucine exchange (P480L) in the short segment connecting D9 and D10 (Figure 1A). P480 is highly conserved within the CIC family (Figure 1B), but the equivalent of R300 is replaced by

tryptophan in a kidney chloride channel (Uchida *et al.*, 1993). P480L, but not R300Q, completely cosegregated with the disease in the Thomsen pedigree (Figure 2), suggesting P480L as the disease-causing mutation.

Expression of human CIC-1

While genetic linkage and disease-associated sequence variations strongly suggest a causal role of the respective gene, a proof requires the demonstration that mutations have the expected functional consequences. We therefore constructed a functional hCIC-1 clone by joining the four missing 5' exons to the partial cDNA obtained previously (Koch *et al.*, 1992). The complete coding sequence is 2964 bp long and codes for a protein of 988 amino acids with a predicted M_r of 110 kDa. It is 88% identical to the rat CIC-1 channel.

For functional expression in *Xenopus* oocytes it was necessary to replace the 5'-untranslated sequence of hCIC-1 by that of the related *Torpedo* chloride channel, CIC-0 (Jentsch *et al.*, 1990). When examined by two-electrode voltage-clamp, currents deactivate at negative voltages and rectify inwardly at positive potentials (Figure 3A). This closely resembles currents of rat CIC-1 (Steinmeyer *et al.*, 1991a), but with the human channel gating at positive voltages was somewhat slower. Expression of hCIC-1 effectively clamped the oocyte resting potential to the chloride equilibrium potential (-30 mV). Replacement of external anions proved its chloride selectivity (Figure 3C). Based on the minor shifts of reversal potentials, iodide and bromide seem rather permeant, but both anions block chloride outward currents in a voltage-dependent manner. The unexpected decrease of inward currents at low extracellular chloride is probably caused by an effect of chloride concentration on gating as observed with CIC-0 (M.Pusch and T.J.Jentsch, unpublished observation).

Characterization of hCIC-1 mutants

Mutations found in MC families (P480L, G230E and R300Q) were introduced into the hCIC-1 cDNA. Equivalent amounts of a 110 kDa protein were made in COS-7 cells

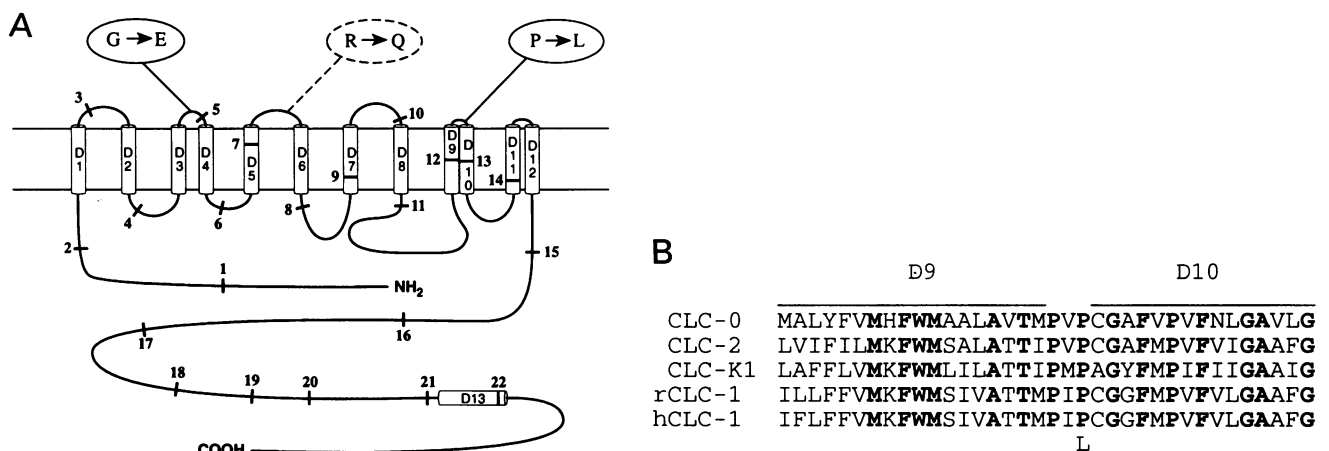


Fig. 1. Exon-intron structure of hCIC-1 and location of mutations. (A) Schematic representation of proposed CIC-1 topology. Putative transmembrane domains are labelled D1 to D12; D13 is a conserved domain located intracellularly (Gründer *et al.*, 1992). Positions of introns are indicated by bars. Locations of mutations found in the Thomsen pedigree (R300Q and P480L substitutions) and in Canadian MC families (G230E; George *et al.*, 1993) are shown. All mutations are located in putative extracellular loops. (B) Homology between different members of the voltage-gated chloride channel family in the region of the Thomsen mutation (P480L). CLC-0, *Torpedo marmorata* electric organ chloride channel; CLC-2, ubiquitous rat chloride channel; CLC-K1, rat kidney chloride channel; rCLC-1, rat skeletal muscle chloride channel; hCLC-1, human skeletal muscle chloride channel. Identical residues are printed in boldface. Putative transmembrane domains D9 and D10 are denoted by lines, and the L at the bottom indicates the mutation found in Thomsen's own family.

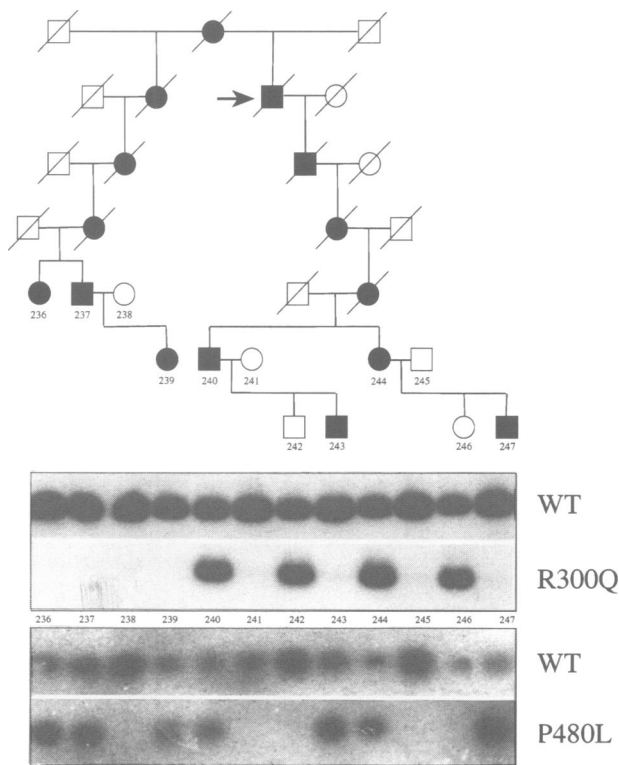


Fig. 2. Segregation of mutations in the Thomsen pedigree. The pedigree of Thomsen is shown on top. Its design (birth order and sex) has been changed to protect patient confidentiality (Koch *et al.*, 1992). The arrow indicates J.Thomsen, who first described the disease (Thomsen, 1876). Unaffected individuals are indicated as empty circles (female) and squares (male), and affected individuals are represented by filled symbols. Symbols are shown above the corresponding Southern lanes. Allele-specific oligonucleotide analysis is shown below. Exons 8 (top two lanes) and 13 (bottom two lanes) were amplified by PCR from genomic DNA of 12 members of Thomsen's family (seven affected and five non-affected individuals, numbered from 236 to 247). Southern analysis of the products used labelled oligonucleotides specific for the R300Q and P480L variants, and for the corresponding WT alleles. Only P480L cosegregated with the disease, suggesting that it causes the disease.

transfected with WT, P480L and G230E mutant hClC-1 (Figure 4). In addition, no significant differences in half-lives could be detected in pulse-chase experiments (data not shown). Thus, these mutations do not interfere with translation efficiency or protein turnover.

When examined in *Xenopus* oocytes, R300Q currents were indistinguishable from WT currents, confirming it as a benign polymorphism. However, insertion of either P480L or G230E (George *et al.*, 1993) abolished chloride currents in the physiological voltage range (-120 to $+80$ mV, data not shown). With P480L, we observed a variable slow activation of a chloride current upon strong hyperpolarization (below -120 mV). By tail current analysis it showed an iodide $>$ chloride selectivity which differs from the chloride $>$ iodide selectivity of WT ClC-1.

Co-expression of WT ClC-1 with Thomsen mutants

Recessive myotonia (Becker type) demonstrates that reducing chloride conductance to $\sim 50\%$ (as expected for heterozygotes) leads to no or minimal physiological consequences (Becker, 1979; Zellweger *et al.*, 1980; Streib and Sun, 1982). Thus, ClC-1 mutants found in dominant

Thomsen's disease must have additional properties to reduce WT ClC-1 currents to lower, pathogenic levels.

We therefore co-injected oocytes with constant amounts of WT and increasing amounts of mutant (P480L or G230E) cRNA. In both cases, chloride currents were suppressed in a dose-dependent manner, with P480L having a more pronounced effect (Figure 5). Similar results were obtained when R300Q and P480L mutants were co-expressed (reflecting the actual situation in the patient from which the library was made).

Though functional expression is not linearly related to the amount of injected RNA (Figure 5, inset), this saturation of expression cannot account for the effects of mutant subunits. The dashed line in Figure 5 indicates the inhibition expected exclusively from competition for expression. It coincides with the nonspecific inhibition exerted by the co-expression of an unrelated membrane protein, the cystic fibrosis transmembrane conductance regulator (CFTR) (Riordan *et al.*, 1989), and is clearly separated from the stronger effects of mutant subunits (especially P480L). Moreover, P480L did not inhibit the expression of cAMP-activated chloride currents mediated by CFTR (data not shown), demonstrating the specificity of the interaction.

The lower degree of inhibition by G230E could be explained by partially functional WT/G230E heterooligomers. We observed subtle, but highly significant changes in channel properties upon G230E/WT, but not P480L/WT, co-expression. Channels activated more slowly at positive potentials (Figure 3B and F), and the iodide block was reduced in the positive voltage range (Figure 3D and E). Both findings strongly suggest functional heterooligomers.

Since iodide preferentially blocks WT channels, currents measured in its presence mainly reflect the number of WT/G230E heterooligomers. With increasing amounts of G230E cRNA, currents pass through a maximum and then decrease again (Figure 6). Thus, functional mutant/WT heterooligomers are formed preferentially at low mutant:WT ratios, while incorporation of a larger number of mutant subunits leads to non-functional channels.

Discussion

The first proof that a genetic defect in a chloride channel causes myotonia was obtained for the recessive myotonic mouse mutant ADR (Steinmeyer *et al.*, 1991b) shortly after the major skeletal muscle chloride channel ClC-1 had been cloned (Steinmeyer *et al.*, 1991a). Linkage studies (Abdalla *et al.*, 1992; Koch *et al.*, 1992) suggested that the human myotonias GM and MC are also due to ClC-1 mutations. Mutations were identified in GM (Koch *et al.*, 1992) and MC (George *et al.*, 1993). While these studies provided strong evidence for an involvement of ClC-1 in both diseases, they did not strictly prove this point as these mutations may be polymorphisms in linkage disequilibrium with the disease-causing mutation. Thus, in studying the functional effects of ClC-1 mutations in MC, the present study provides the first unambiguous proof that ClC-1 mutations cause dominant myotonia (Thomsen's disease). By studying Thomsen's own family, we have identified the 'original' mutation in Thomsen's disease.

The mutation identified here (P480L) and that described in Canadian families (G230E) (George *et al.*, 1993) both change amino acids with α -helix and β -sheet breaking

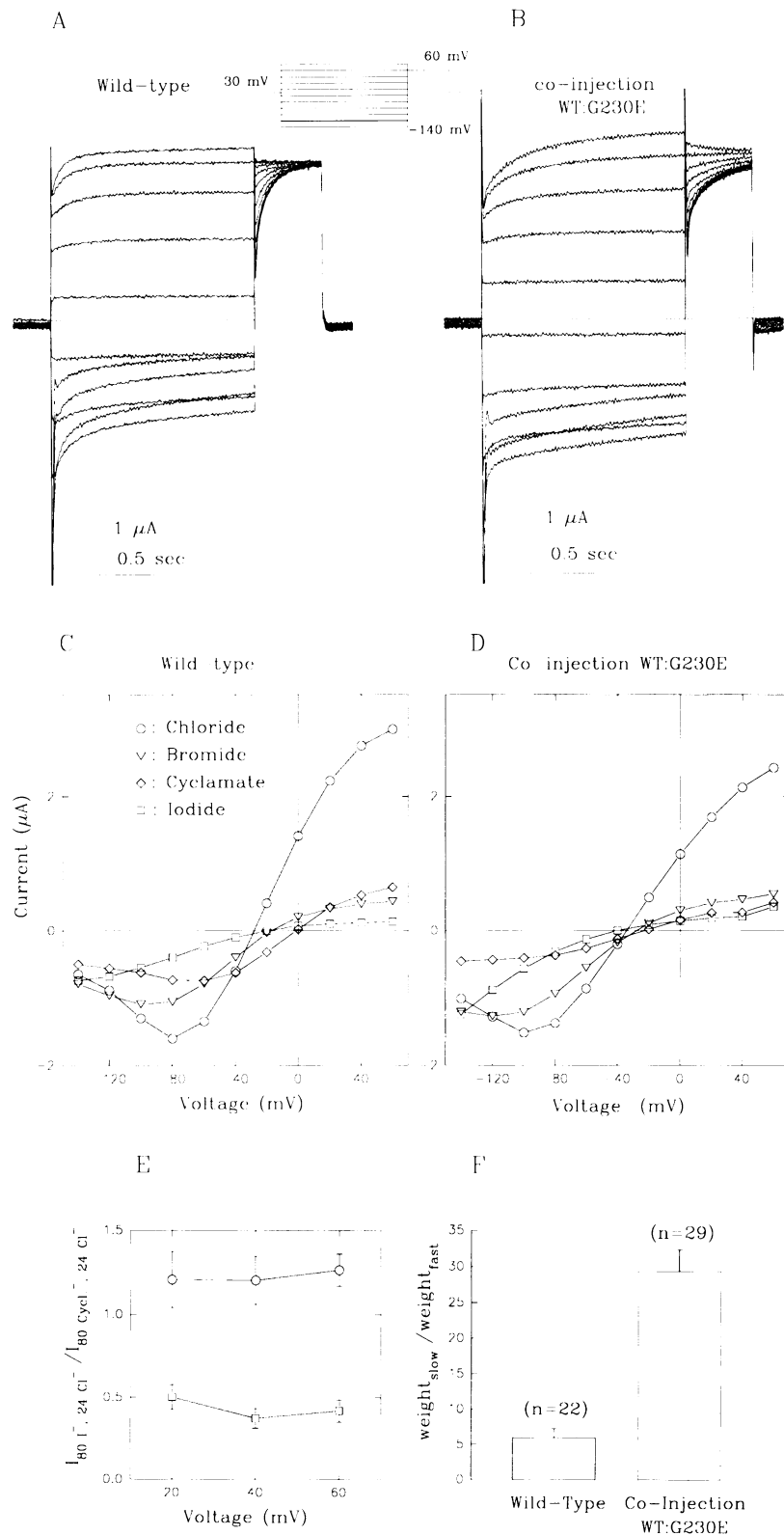


Fig. 3. Comparison between WT hClC-1 and WT/G230E heterooligomers expressed in *Xenopus* oocytes. (A and B) Typical voltage clamp traces of WT and heteromeric channels, respectively; the clamp program is shown in the inset. (C) (WT) and (D) (WT/G230E) current-voltage relationships in the presence of 105 mM chloride, and in saline where 80 mM chloride was replaced by bromide, iodide or cyclamate. (E) Difference in iodide block between WT (□) and WT/G230E (○) channels; ratios of currents in the presence of 80 mM iodide or cyclamate measured at positive voltages where iodide block is strongest for WT hClC-1. The mean current of at least five oocytes is shown (error bars show SEM). (F) Kinetic differences between WT channels and WT/G230E heterooligomers (3:1 ratio of RNAs); to estimate the relative contributions of slow and fast activation at +60 mV, the sum of two exponentials [of the form $a_0 + w_1k_1\exp(-k_1t) + w_2k_2\exp(-k_2t)$, ($k_1 < k_2$)] was fitted to the data, and the ratio (w_1/w_2) of the respective weights (areas under the exponential curves) was calculated. Time constants ranged between 40 and 80 ms for the fast component, or between 300 and 700 ms for the slow component, with no difference between WT and co-injection. *n*, number of oocytes; error bars indicate SEM.

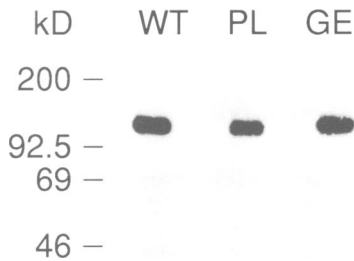


Fig. 4. Quantification of WT and mutant hCLC-1 proteins expressed in COS-7 cells. WT, P480L mutant (PL) and G230E mutant (GE) hCLC-1 channels were epitope-tagged and transiently expressed in COS-7 cells. Comparable amounts of a ~110 kDa protein were detected by sequential immunoprecipitation and immunoblotting using an epitope-specific monoclonal antibody.

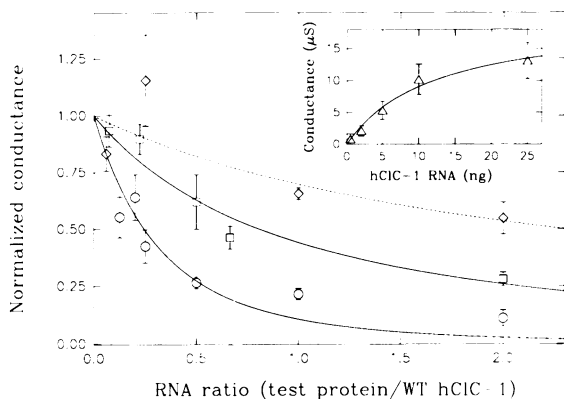


Fig. 5. Analysis of dominant negative effects. Effects of increasing amounts of P480L (○) and G230E (□) cRNA on currents expressed from constant amounts of WT hCLC-1 RNA (typically 10 ng/oocyte). (◇), effect of increasing amounts of CFTR RNA on hCLC-1 currents (control). Conductance coincides with the decrease in conductance (dashed line) predicted exclusively from the saturation of expression observed with hCLC-1 (inset). The solid line in the inset represents a Michaelis-Menten fit which gave half-maximal conductance at 12 ng RNA. Conductance after 2 days at -20 mV (normalized to WT conductance) is shown as a function of the mutant/WT or CFTR/WT RNA ratio. Points represent averaged normalized values from three titration experiments for hCLC-1 mutants (three to 15 oocytes, three batches of oocytes, three or more batches of RNA), or from one titration experiment for CFTR. Error bars indicate SEM. Lines represent fits according to a simple model in which incorporation of one mutated subunit suffices to inactivate functionally a multimeric channel complex (described in detail in Materials and methods). Taking saturation into account, these fits estimate the number of subunits (k) as 3.7 ± 0.4 for P480L and 1.7 ± 0.2 for G230E.

potential in segments thought to connect transmembrane spans. Their replacement may lead to a distortion of channel geometry. The predicted loop between domains D9 and D10, where Thomsen's mutation is located, is especially short. This could explain the more pronounced functional effects of P480L. On the other hand, the negative charge introduced in the G230E mutant may explain the altered voltage-dependent iodide block observed in heterooligomers.

With the P480L mutant no chloride currents were detected at physiological voltages, as expected from a mutation causing myotonia. However, upon strong hyperpolarization, we observed a variable slow development of a current which was generally absent in control oocytes. Its ion selectivity (iodide > chloride) is different from that of WT ClC-1 (which is blocked by iodide), but coincides with that of an

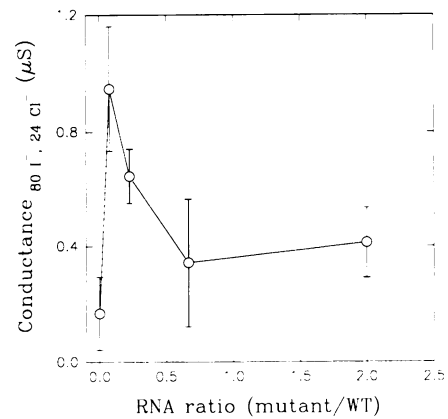


Fig. 6. Expression of functionally altered channels as a function of G230E/WT RNA ratio. Slope conductance (at -20 mV) in ND96 with 80 mM chloride replaced by iodide. Since this iodide concentration preferentially blocks WT channels, currents represent mainly WT/G230E heterooligomers. Oocytes were injected with constant amounts of WT (~10 ng/oocyte) and increasing amounts of mutant RNA. The mean current of four or five oocytes is shown. Error bars indicate SEM. Four independent titration experiments (four batches of oocytes, three batches of RNA) yielded current maxima between 0.1 and 0.8 of mutant:WT RNA concentrations. The predicted decrease of heteromers at higher mutant RNA concentration due to nonspecific saturation of expression (Figure 5, inset) is still negligible for RNA ratios of <2.

endogenous oocyte hyperpolarization-activated chloride current (Kowdley *et al.*, 1994). Thus it may either represent some nonspecific effect on the *Xenopus* channel, or P480L homooligomers form channels with grossly changed voltage-dependence and ion selectivity. Interestingly, overexpression of I_{SK} , a protein thought to form potassium channels (Takumi *et al.*, 1988), leads to similar hyperpolarization-activated chloride currents in *Xenopus* oocytes (Attali *et al.*, 1993), as does the expression of phospholemman, a protein also having just a single transmembrane segment (Moorman *et al.*, 1992). This seems to support the first hypothesis.

Both MC mutations showed a dominant negative effect in the oocyte, but the degree of inhibition was much stronger with the original Thomsen mutation. While currents were reduced to <10% in a situation resembling WT/P480L heterozygosity, they decreased to only ~35% with WT/G230E co-expression (if corrected for saturation of translation). In individuals heterozygous for recessive myotonia (GM), chloride conductance levels are expected to be 50% of normal without having functional consequences. However, there are reports that some GM heterozygotes also present with mild symptoms (Becker, 1979; Zellweger *et al.*, 1980; Streib and Sun, 1982). On the other hand, reducing chloride conductance to ~25% using chloride channel inhibitors leads to myotonic symptoms *in vitro* (Kwiecinski *et al.*, 1988). Thus, if the *Xenopus* oocyte expression system is representative of the *in vivo* situation, the dominant negative effect of the G230E mutation may be just sufficient to explain the dominant pattern of inheritance. The altered kinetic properties of WT/G230E heteromeric channels, which will mediate the majority of chloride conductance remaining in heterozygous patients, may also contribute to a lengthening of action potentials.

Our experiments suggest that ClC channels are (homo)oligomers whose function will be destroyed by the incorporation of mutant subunits. The extent of the reduction of chloride conductance will depend on the number of

subunits and the effect mutant subunits have in such a complex. In the most simple model, which assumes that a single mutant subunit suffices to inactivate the complex completely, a dimeric channel should yield a quarter of the WT current under conditions found in heterozygous patients (1:1 ratio of WT:mutant RNAs). With a tetramer, the current will decrease to 1/16. Thus, titration experiments may give a rough estimate of subunit stoichiometry.

Surprisingly, such an analysis (Figure 5) predicts at most a dimer for the G230E mutant, whereas a model with four subunits is best suited to explain the results with P480L. This apparent contradiction can be resolved by recognizing that these experiments will only give a lower limit: depending on the mutation, more than one mutant subunit may be necessary to inhibit channel function completely, and WT/mutant heterooligomers may still have channel activity. In fact, CIC-1 kinetics and selectivity were changed when co-expressed with the G230E mutant, strongly suggesting functional WT/G230E heterooligomers. This fully agrees with the less pronounced dominant negative effect of the G230E mutant.

The analysis of WT/G230E currents independently proves that more than two subunits form a functional channel. In the case of a dimeric channel, a constant number of functionally altered WT/G230E dimers would be reached with constant amounts of WT and increasing amounts of mutant RNA. Currents measured in the presence of iodide, which preferentially blocks WT channels, allowed us to estimate the amount of functional WT/G230E heterooligomers. These currents steeply increased with low amounts of G230E RNA, but rapidly decreased at higher mutant RNA concentration. This suggests that functional heterooligomers are only formed at a low ratio of mutant to WT subunit concentrations. Further incorporation of mutant subunits into the channel complex destroys channel activity, leading to the dominant negative effect. This reasoning implies that the minimum number of subunits in a CIC-1 channel is three. Importantly, and in contrast to the analysis of the extent of dominant negative effects, this conclusion does not depend on the assumption that WT and mutant channels are synthesized at equal efficiencies. The homologous *Torpedo* channel CIC-0 is believed to have a 'double-barrelled' structure with two independent, identical pores (Hanke and Miller, 1983; Bauer *et al.*, 1991). Thus, for symmetry reasons, it is tempting to assume that CIC-1 channels are tetrameric (consistent with the P480L titration experiment indicating 3.7 ± 0.4 subunits).

It would be valuable to complement our studies with single channel measurements. However, noise analysis estimated hCIC-1 single channel conductance to be ~ 1 pS (Pusch *et al.*, 1994). This effectively precludes detailed single-channel analysis of hCIC-1 and its mutants and eliminates several candidate channels hypothesized to cause myotonia (Fahlke *et al.*, 1993; Weber-Schürholz *et al.*, 1993).

In summary, our work proves that various mutations in human CIC-1 cause dominant (Thomsen) myotonia. Our data are consistent with a tetrameric structure of CIC-1. In this model, the incorporation of a single mutant P480L subunit is sufficient to destroy channel activity. With G230E, two or more mutant subunits are needed for inactivation, while incorporation of only one mutant leads to functionally altered channels. This multimeric structure is likely to apply for other members of this gene family as well. Dominant negative mutants like those described here may be useful

tools to knock out endogenous CIC channels in either cultured cells or organisms.

Materials and methods

Genomic cloning of hCIC-1

A commercial human genomic DNA library (λ FIXII, Stratagene) was used to determine exon–intron boundaries of the hCIC-1 gene, and a genomic library in λ FIXII was constructed with lymphocyte DNA from a myotonic member of the Thomsen pedigree (patient #240, Figure 2). Libraries were screened with the partial hCIC-1 cDNA clone pL7 (Koch *et al.*, 1992) as a probe using standard methods (Sambrook *et al.*, 1989). Phage inserts were released with *NorI* and were subcloned into pBluescript.

Sequencing of genomic clones and identification of mutations

Genomic clones were mapped to specific parts of the cDNA by hybridization and were sequenced using synthetic oligonucleotide primers complementary to exonic sequence of human CIC-1 (or rat CIC-1 for the 5' end). Exon–intron boundaries were identified by computer alignments with rat CIC-1 (GenBank accession no. X62894) and partial hCIC-1 clone pL7 (GenBank accession no. M97820). It will be described elsewhere in detail (C. Lorenz, K. Steinmeyer and T.J. Jentsch, in preparation). Intronic primers were used to sequence the adjacent exons. This revealed a G to A exchange at position 899 (exon 8), leading to the R300Q exchange; and a C to T transition at bp 1439 (exon 13), leading to the P480L exchange. These mutations were on different λ clones containing both regions, and thus stem from different alleles (consistent with the segregation in the pedigree).

Construction of a complete hCIC-1 cDNA sequence

The first four exons of hCIC-1 were amplified by PCR from a genomic clone containing the 5' end of the cDNA using the following protocol: 94°C for 2 min, then 15 cycles of 94°C for 1 min, 46°C for 1.5 min and 72°C for 1.5 min. For the recombinant PCR used to link these fragments the annealing temperature was 50°C. The resulting fragment was cut with *SphI* and *BstXI* and ligated to the 5' located *BstXI* site of cDNA clone pL7. The following oligonucleotide primers were used: exon 1: upstream primer, 5'-TGCACCTCACCTGCTTC-3', downstream primer, 5'-CTGTGTGGGGTGGACGTT-3'. Exon 2: upstream primer, 5'-GTCCACCCACACAGATTTATGGCCATCAC-3', downstream primer, 5'-CTTGACATTAGATAAGT-3'. Exon 3: upstream primer 5'-ATTCTAAATGTC-AAGATTGTATCCACCGCC-3', downstream primer, 5'-CCTGAAGGCTTTTGGCAC-3'. Exon 4: upstream primer, 5'-CCAAAAGCC-TTCAGGCCTACAAGTGGTCT-3', downstream primer, 5'-GGGATCCAGAGCCAACAGCCTGGGGAGAG-3'. The sequence of the complete human CIC-1 cDNA has been submitted to the EMBL/GenBank database, accession no. Z25884.

Site directed mutagenesis

Point mutations were introduced into the respective cDNAs by recombinant PCR. Briefly, two fragments were amplified with primers containing the desired mutation in a short overlapping region, joined by recombinant PCR, digested with appropriate restriction endonucleases and ligated into the cDNA. PCR-derived fragments were entirely sequenced.

Allele-specific oligonucleotide hybridization

Genomic DNA (200–500 ng) from individual members of the Thomsen family was amplified using equimolar concentrations of primers (exon 8: upstream primer 5'-TCCTTAGGTCCAAGCAGT-3', downstream primer 5'-AGAGTTTTCTCTGCACC-3'; exon 13: upstream primer 5'-CTT-CAGCTTGCCATCGTT-3', downstream primer 5'-ACTACTTATGCTCTGAAG-3'). Amplifications were performed as follows: 94°C for 5 min, then 50 cycles of 94°C for 1 min, 65°C for 1.5 min and 72°C for 1.5 min. Reaction products were subjected to Southern analysis using allele-specific oligonucleotides (11mers) end-labelled with 32 P as probes (exon 8: normal allele, 5'-TGTTCCGGAAGT-3'; mutant allele, 5'-TGTTCCAGAACT-3'. Exon 13: normal allele, 5'-CATACCCTGCG-3'; mutant allele, 5'-CATACTCTGCG-3'). Prehybridization and hybridization were performed at 18°C (for exon 8) or at 25°C (for exon 13) in $5 \times$ SSC. Filters were washed twice with $5 \times$ SSC at the hybridization temperature and processed for autoradiography.

Western analysis of transfected cells

hCIC-1 WT, P480L and G230E mutant proteins were epitope-tagged by inserting oligonucleotides encoding the haemagglutinin epitope (YPYDVPDYA) of influenza virus into the respective cDNA at the 3' *Apal* site (after conserved domain D13; this has no influence on functional expression of WT CIC-1). COS-7 cells were transfected with $1 \mu\text{g/ml}$ of

these constructs which had been cloned into the pcDNA1 vector (Invitrogen) using the calcium phosphate precipitation method (Chen and Okayama, 1987). 48 h after transfection, cells were washed twice with ice-cold phosphate buffered saline and were extracted for 30 min on ice with lysis buffer (50 mM Tris-HCl, pH 8.0, 120 mM NaCl, 1% NP-40, 10% glycerol, 5 mM DTT, 1 mM EGTA, 30 µg/ml aprotinin, 1 mM PMSF). Extracts were cleared by centrifugation for 30 min at 12 000 g and +4°C. hClC-1 was immunoprecipitated with monoclonal antibody 12CA5 recognizing the haemagglutinin epitope of the influenza virus (Wilson *et al.*, 1984) for 3 h using protein A-Sepharose (Pharmacia). Immunoprecipitates were separated on a 10% polyacrylamide-SDS gel and transferred to a nitrocellulose filter which was sequentially incubated with the monoclonal antibody and ¹²⁵I-labelled protein A and then exposed on Kodak XAR-5 film.

Electrophysiological methods

Capped mRNA was transcribed by T7 or T3 RNA polymerase after linearization with *Xba*I or *Nor*I, depending on the construct. 5–10 ng cRNA was injected into *Xenopus* oocytes prepared and handled as described (Jentsch *et al.*, 1990). Oocytes were kept and analysed in ND96 saline (96 mM NaCl, 2 mM KCl, 1.8 mM CaCl₂, 1 mM MgCl₂, 5 mM HEPES, pH 7.4), or in ND96 in which 80 mM chloride was replaced by the anions indicated in the figures. Standard two-electrode voltage-clamp measurements were performed 2 days after injection at room temperature (20–24°C) using pCLAMP software (Axon Instruments).

Analysis of titration experiments

To analyse titration experiments exploring the dominant negative effects of mutants (Figure 5), we assumed the following simplified model: only complete channels with a fixed stoichiometry are formed with no preference given to WT or mutant subunits during assembly. Further, we assumed that a single mutant subunit totally inhibits channel function in such a complex. This assumption gives a lower limit for the number of subunits, because more than one subunit may be needed to inhibit the complex (as with G230E). If we have n_W WT and n_M mutant subunits, the probability, P_k , of finding a WT homooligomer is $1/(1 + \alpha)^k$, where α is the ratio n_M/n_W and k is the number of subunits. The absolute number of homooligomeric WT channels, N_k , is then $n_W/k(1 + \alpha)^{k-1}$. Therefore, assuming that protein synthesis is proportional to the amount of RNA, the conductance G is $G_0/(1 + \alpha)^k$, where G_0 is the conductance observed without the mutant channel. Equally efficient synthesis of WT and mutant subunits is suggested by Figure 4. If saturation is taken into account, the above value of G must be multiplied by a Michaelis-Menten type factor, $(1 + \beta)/(1 + \beta + \alpha)$, where $\beta = n_{1/2}/n_W$, where $n_{1/2}$ is the amount of RNA leading to half-maximal expression. $n_{1/2}$ was experimentally determined as 12 ng (Figure 5, inset).

Acknowledgements

We thank Christine Schmekal for technical assistance, Franco Conti and Peking Fong for reading the manuscript, and John R. Riordan for the CFTR cDNA. This work was supported, in part, by the Bundesministerium für Forschung und Technologie, the Deutsche Forschungsgemeinschaft, the Fonds der Chemischen Industrie, and the US Muscular Dystrophy Association.

References

- Abdalla, J.A., Casley, W.L., Cousin, H.K., Hudson, A.J., Murphy, E.R.G., Cornéilis, F.C., Hashimoto, L. and Ebers, G.C. (1992) *Am. J. Hum. Genet.*, **51**, 579–584.
- Attali, B., Guillemare, E., Lesage, F., Honoré, E., Romey, G., Lazdunski, M. and Barhanin, J. (1993) *Nature*, **365**, 850–852.
- Bauer, C.K., Steinmeyer, K., Schwarz, J.R. and Jentsch, T.J. (1991) *Proc. Natl Acad. Sci. USA*, **88**, 11052–11056.
- Becker, P.E. (1977) *Myotonia Congenita and Syndromes Associated with Myotonia*. Thieme, Stuttgart.
- Becker, P.E. (1979) *Hum. Genet.*, **46**, 325–329.
- Bretag, A.H. (1987) *Physiol. Rev.*, **67**, 618–725.
- Bryant, S.H. and Morales-Aguilera, A. (1971) *J. Physiol. (Lond.)*, **219**, 367–383.
- Cannon, S.C. and Strittmatter, S.M. (1993) *Neuron*, **10**, 317–326.
- Chen, C. and Okayama, H. (1987) *Mol. Cell. Biol.*, **7**, 2745–2752.
- Cooper, E., Couturier, S. and Ballivet, M. (1991) *Nature*, **350**, 235–238.
- Cummins, T.R., Zhou, J., Sigworth, F.J., Ukomadu, C., Stephan, M., Ptáček, L. and Agnew, W.S. (1993) *Neuron*, **10**, 667–678.
- Fahlke, C., Zachar, E. and Rüdel, R. (1993) *Neuron*, **10**, 225–232.
- Franke, C., Iaizzo, P.A., Hatt, H., Spittelmeister, W., Ricker, K. and Lehmann-Horn, F. (1991) *Muscle Nerve*, **14**, 762–770.
- George, A.L., Jr, Crackower, M.A., Abdalla, J.A., Hudson, A.J. and Ebers, G.C. (1993) *Nature Genet.*, **3**, 305–310.
- Gisselmann, G., Sewing, S., Madsen, B.W., Mallart, A., Angaut-Petit, D., Müller-Holtkamp, F., Ferrús, A. and Pongs, O. (1989) *EMBO J.*, **8**, 2359–2364.
- Gründer, S., Thiemann, A., Pusch, M. and Jentsch, T.J. (1992) *Nature*, **360**, 759–762.
- Hanke, W. and Miller, C. (1983) *J. Gen. Physiol.*, **82**, 25–42.
- Jentsch, T.J., Steinmeyer, K. and Schwarz, G. (1990) *Nature*, **348**, 510–514.
- Koch, M.C., Steinmeyer, K., Lorenz, C., Ricker, K., Wolf, F., Otto, M., Zoll, B., Lehmann-Horn, F., Grzeschik, K.-H. and Jentsch, T.J. (1992) *Science*, **257**, 797–800.
- Kowdley, G.C., Ackerman, S.J., John, J.E., Jones, L.R. and Moorman, J.R. (1994) *J. Gen. Physiol.*, in press.
- Kwiecinski, H., Lehmann-Horn, F. and Rüdel, R. (1988) *Muscle Nerve*, **11**, 576–581.
- Langosch, D., Thomas, L. and Betz, H. (1988) *Proc. Natl Acad. Sci. USA*, **85**, 7394–7398.
- Lipicky, R.J., Bryant, S.H. and Salmon, J.H. (1971) *J. Clin. Invest.*, **50**, 2091–2103.
- MacKinnon, R. (1991) *Nature*, **350**, 232–235.
- McClatchey, A.I., Van den Bergh, P., Pericak-Vance, M.A., Raskind, W., Verellen, C., McKenna-Yasek, D., Rao, K., Haines, J.L., Bird, T., Brown, R.H. and Gusella, J.F. (1992) *Cell*, **68**, 769–774.
- Mehrke, G., Brinkmeier, H. and Jockusch, H. (1988) *Muscle Nerve*, **11**, 440–446.
- Moorman, J.R., Palmer, C.J., John, J.E., Durieux, M.E. and Jones, L.R. (1992) *J. Biol. Chem.*, **267**, 14551–14554.
- Müller-Hill, B., Crapo, L. and Gilbert, W. (1968) *Proc. Natl Acad. Sci. USA*, **59**, 1259–1264.
- Ptáček, L.J., George, A.L., Griggs, R.C., Tawil, R., Kallen, R.G., Barchi, R.L., Robertson, M. and Leppert, M.F. (1991) *Cell*, **67**, 1021–1027.
- Pusch, M., Steinmeyer, K. and Jentsch, T.J. (1994) *Biophys. J.*, **66**, 149–152.
- Riordan, J.R., Rommens, J.M., Kerem, B.S., Alon, N., Rozmahel, R., Grzelczak, Z., Zielenski, J., Lok, S., Plavsik, N., Chou, J.L., Drumm, M.L., Iannuzzi, M.C., Collins, F.S. and Tsui, L.C. (1989) *Science*, **245**, 1066–1073.
- Rojas, C.V., Wang, J., Schwartz, L.S., Hoffman, E.P., Powell, B.R. and Brown, R.H. (1991) *Nature*, **354**, 387–389.
- Rüdel, R. and Lehmann-Horn, F. (1985) *Physiol. Rev.*, **65**, 310–356.
- Rüdel, R., Ricker, K. and Lehmann-Horn, F. (1988) *Muscle Nerve*, **11**, 202–211.
- Sambrook, J., Fritsch, E.F. and Maniatis, T. (1989) *Molecular Cloning: A Laboratory Manual*. 2nd edn. Cold Spring Harbor Laboratory Press, Cold Spring Harbor, NY.
- Steinmeyer, K., Orland, C. and Jentsch, T.J. (1991a) *Nature*, **354**, 301–304.
- Steinmeyer, K., Klocke, R., Orland, C., Gronemeier, M., Jockusch, H., Gründer, S. and Jentsch, T.J. (1991b) *Nature*, **354**, 304–308.
- Streib, E.W. and Sun, S.F. (1982) *Muscle Nerve*, **5**, 179–181.
- Takumi, T., Ohkubo, H. and Nakanishi, S. (1988) *Science*, **242**, 1042–1045.
- Thiemann, A., Gründer, S., Pusch, M. and Jentsch, T.J. (1992) *Nature*, **356**, 57–60.
- Thomsen, J. (1876) *Arch. Psychiatr. Nervenkrankh.*, **6**, 702–718.
- Uchida, S., Sasaki, S., Furukawa, T., Hiraoka, M., Imai, T., Hirata, Y. and Marumo, F. (1993) *J. Biol. Chem.*, **268**, 3821–3824.
- Unwin, N., Toyoshima, C. and Kubalek, E. (1988) *J. Cell Biol.*, **107**, 1123–1138.
- Weber-Schürholz, S., Wischmeyer, E., Laurien, M., Jockusch, H., Schürholz, T., Landry, D.W. and Al-Awqati, Q. (1993) *J. Biol. Chem.*, **268**, 547–551.
- Wilson, I.A., Niman, H.L., Houghten, A.R., Cherenon, M.L., Connolly, M.L. and Lerner, R.A. (1984) *Cell*, **37**, 767–778.
- Zellweger, H., Pavone, L., Biondi, A., Cimino, V., Gulett, F., Hart, M., Ionescu, V., Mollica, F. and Schieken, R. (1980) *Muscle Nerve*, **3**, 176–180.

Received on October 6, 1993; revised on November 29, 1993